ARCHITECTURAL SCIENCE REVIEW

Solar obstruction assessment model for densely forested urban environments

Alejandro Mesa*, Mariela Arboit and Carlos de Rosa
Laboratorio de Ambiente Humano y Vivienda, Instituto de Ciencias Humanas, Sociales y Ambientales, CONICET, C. C.131, 5500 Mendoza, Argentina

Cities display an array of microclimates closely related to the composition of their surfaces and the relationships among their structures. The effect of the shadow cast by a high-rise building is a simple case of this situation. The incidence of the shadow on other buildings or urban spaces can be positive or negative, according to the bioclimatic requirements of the place and season. The understanding of the cause of these effects is key information that helps when planning new urban complexes or refurbishing existing ones. In climates with high space heating demands, precise assessment of the available solar resource is of vital importance. In order to cope with this requirement, a predictive methodology based on the processing of digital images of the sectors to be analysed has been developed. Although there are other computational methods available for this task, they are not adequate to the assessed areas' features, because of the relevant incidence of urban forest in this case.

Keywords: Solar component radiation; solar obstruction; urban structure

INTRODUCTION

When the feasibility of a bioclimatic design for a new building or the recycling of an existing one is analysed, a precise knowledge of the available solar resource is essential, particularly in consolidated urban environments where the specific features of the building structure significantly condition access to, and the availability of, climatic resources.

The impinging radiation balance on a given building is different every time the features of its neighbouring environment change (Temps and Coulson, 1977; Robinson *et al.*, 2003; Robinson and Stone, 2004). On a clear day, the impact of reflected radiation from an insolated vertical or horizontal surface can significantly increase the radiation availability impinging on an opposite surface. Vertical and horizontal surfaces are considered as potential energy sources for buildings, particularly in regions with clear skies and a generous solar resource (Hay, 1979; Klucher, 1979; Randall *et al.*, 1981).

The urban space assessed is Mendoza's Metropolitan Area (MMA), a conglomerate reaching close to a million people, set on the Andean foothills of Mendoza's province in the arid zone of central-western Argentina. It has been integrated by the long-time conurbation process of six former town cores: Las Heras to the north; Mendoza's Capital and Godoy Cruz at the centre; Guaymallén to the East; and Maipú and Lujan to the south (Figure 1).

MMA features a strong presence of forested urban spaces and dense tree alignments along the city-block's structure conforming with real-time 'green screens' (Figure 2), thus transforming the region's desert nature into an oasis appropriate for human activities.

The evaluation of existing programmes based on the analysis of geometrical models, which allowed for the calculation of the impinging radiation's value on the different outer surfaces of a building (Ecotect, Radiance, Townscope), led to the conclusion that their results did not adhere to the reality of the local environments, where the incidence of urban forest is highly significant.

Since a graphic-computational model developed by previous research (Mesa *et al.*, 2000) only takes into account the solar radiation's direct component, it was deemed necessary to advance on the development of a methodology that could calculate the magnitude of each of the radiation's components (direct, diffuse and reflected) impinging on buildings inserted in consolidated urban environments (Robinson *et al.*, 2003; Robinson and Stone, 2004). Given they reach a significant weight even on clear days, still their features make them difficult to quantify.

With reference to the features of MMA's existing urban forest, there is available information from former studies of the research group on the seasonal solar permeability of the most representative tree species and the availability of natural light in the urban area. It provides valuable complementary data for the attainment of the studies' objectives

*Corresponding author: *Email*: amesa@lab.cricyt.edu.ar

doi:10.3763/asre.2009.0047 ISSN: 0003-8628 (print), 1758-9622 (online) www.earthscan.co.uk/journals/asre

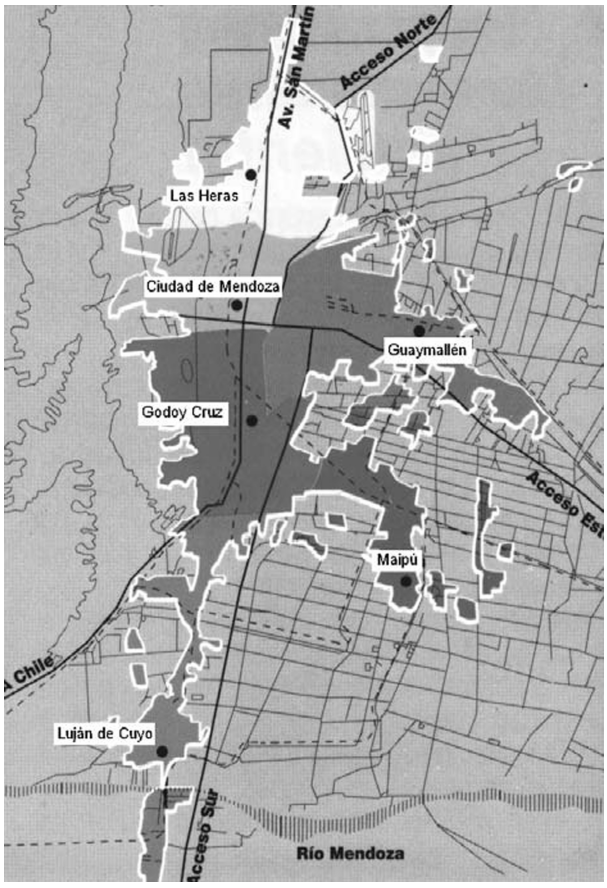

Figure 1 | Political structure of Mendoza's Metropolitan Area

(Cantón *et al.*, 1994, 2001, 2003; Córica *et al.*, 2006a, b, 2007; Martinez *et al*., 2006).

METHOD'S DESCRIPTION

The methodology developed can calculate the sky dome's percentage free of obstructing elements (opaque or permeable) and the potentially reflecting solar radiation areas from digital photo images captured from the viewpoint (centre) of the area to be evaluated.

Given the complex array of features of each specific site, the results obtained will not match closely, but their statistical treatment will allow them to be identified, among the repetitive features of each situation, the main incident variables, thus allowing the characterization of the different urban sectors.

INDICATOR'S DEFINITION

Taking into account the incidence of the nearby environment on the potential collection of a building's vertical surface, four main radiation sources are identified:

Figure 2 | Typical image of MMA green corridors

1 Direct component DC: a parallel radiation prism, whose direction and intensity vary according to the relative solar position on its path in front of a surface.
2 Diffuse component dC: incoming radiation from the sky dome (without considering DC), the result of atmospheric dispersion and the reflection of clouds.
3 Terrain reflected component TRC: incoming radiation from the reflecting surfaces of the nearby environment below the horizon line.
4 Obstacles reflected component ORC: incoming radiation reflected by the surface of opaque obstructions (solid or permeable) above the horizon line (Figure 3).

In order to perform calculations, each one of them will be broken down into its different existing components (paving type, tree species) or included in a group if determined by the case. In this analysis stage, five indicators were determined; they describe the existing variables in the considered urban environments.

1 Sky: Sky dome area free of all obstacles.
2 SOAB1: Obstruction area produced by solid elements of the evaluated construction (overhangs, protrusions).
3 SOAB2: Areas of obstruction caused by solid components of other buildings.
4 POA: Areas of obstruction caused by permeable components (urban trees).
5 PRHA: Potentially reflecting horizontal areas. The indicator could be broken down to the existing materials at each analysed sector (paving type, asphalt carpet).

IMAGE CAPTURES

In order to obtain reliable data, putting aside any possible human error, the use of digital photo images in JPG format

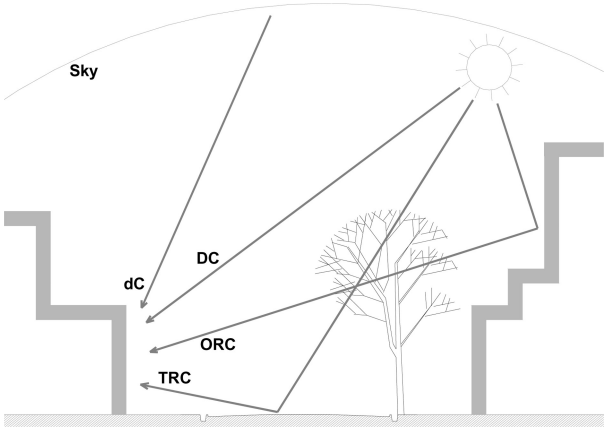

Figure 3 | Solar radiation components impinging on a building in consolidated urban environments

was implemented, as they can be analysed with any image-processing software.

The chosen alternative for their capture was the utilization of hemispheric photographs. They present the projection of a hemispheric surface as a plane surface (extreme capture angle: 180°), thus obtaining a permanent register of the site. It can subsequently be analysed in order to determine which parts of the sky are visible, which objects are secondary reflection sources, and which surrounding urban environment is obstructing (Roxburgh and Kelly, 1995).

The fundamental steps for correct image capture can be summed up as the best fit of these pairs: camera-tripod; position and horizontal levelling of the camera at an adequate height from the floor and lens orientation, making sure that any obstacle alien to the analysed environment stays out of the lens' vision angle.

Later, the images should be analysed using image-processing software, based on the evaluated geometry, to obtain visibility values of the sky and obstructions of it, to calculate solar radiation regimes, the differences in architectural morphology, utilized materials (albedo) and those characterizing the urban forest (species, location and age).

In the described case the following equipment was used: a Nikon Cool Pix 5400 digital camera, an image sensor, a type CCD image sensor with 5.26MP total resolution, 5.1MP effective resolution, 5.8–240mm focal distance (equivalent to 35mm: 28–116mm), 4× – digital 4× optical zoom, (W-T) f 2.8 – f 4.6 maximum aperture. The camera was equipped with a Nikon FC E9 type converter, 'fish-eye' special function, 0.2 enlargement and 4 group(s)/6 elements(s) lens construction. The shutter speed and the aperture did not affect the results. To avoid imprecision, the whole equipment was mounted on an adjustable tripod.

In order to obtain an adequate overview of the analysed sectors, the photographic registers were put at a 5-m distance from the image's centre to obtain, through the overlapping of photographs, the total register of the evaluated area (Figure 4).

Since the study's goal is the assessment of the solar radiation impinging on potentially collecting vertical surfaces, the photo images are captured with the camera's objective aiming north, given that for the analysed latitude, the north receives the maximum quantity of radiation during the heating season. The camera lens' target is determined by aiming it on the centre point of the potential collecting surface being studied.

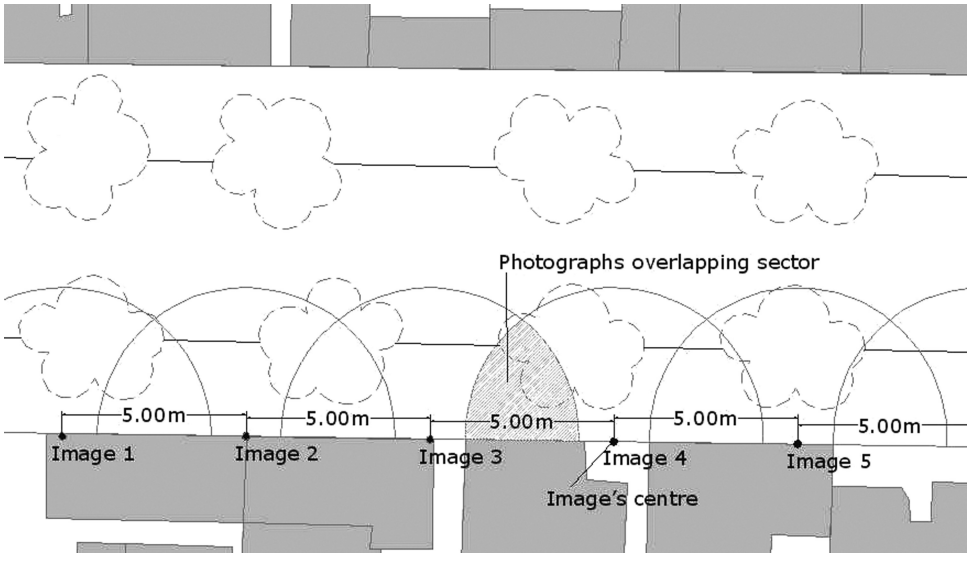

Figure 4 | Location of image capture points at the evaluated environments

DEFINITION OF AN ANGULAR GRID FOR THE DETERMINATION OF OBSTRUCTIONS

Captured from a viewpoint perpendicular to the ground, the hemispheric projection provides a 180° vision field resulting in the complete view of the sky dome in all directions, with the zenith at the image's centre and the horizon lines on its perimeter. The angle between the zenith and any point of the hemispheric projection is directly proportional to the distance along a radial axis within the image.

As in this evaluated case the digital image's axis is not perpendicular to the ground but parallel to it, the need to determine an analytical grid on which the different angular areas could be traced was realized (Figure 5).

In the case of the resulting angular grid, its centre point corresponds to the equator's direction (north in the Southern Hemisphere) and the horizontal line determines the theoretical horizon; above it, the area of the sky dome extends and below it so does the quarter corresponding to the ground's dome. It is divided by 10° contours in height and 15° in azimuth, which gives 216 equivalent angular sectors.

In Figure 4 the A and B sectors correspond to equivalent angular areas limited by a 20° altitude and 30° azimuths. In order to complete the grid, the various lines corresponding to the location's solar paths must be drawn on it; in this case, −32°40′ latitude (Figure 6).

Referring back to the analytical angular grid and the typical sun paths of the stereographic solar chart, it is possible to evaluate the daily periods in each yearly season when the sun is totally free from opaque or permeable obstructions (nearby buildings, urban trees).

From each case's synthesis schemes, the necessary information to determine the potential availability of the solar resource in its different components, direct, diffuse and reflect, is drawn (Figure 7).

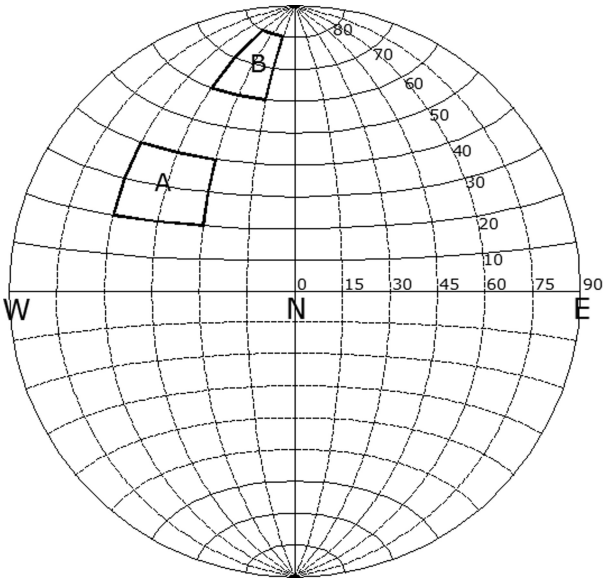

Figure 5 | Analysis grid scheme

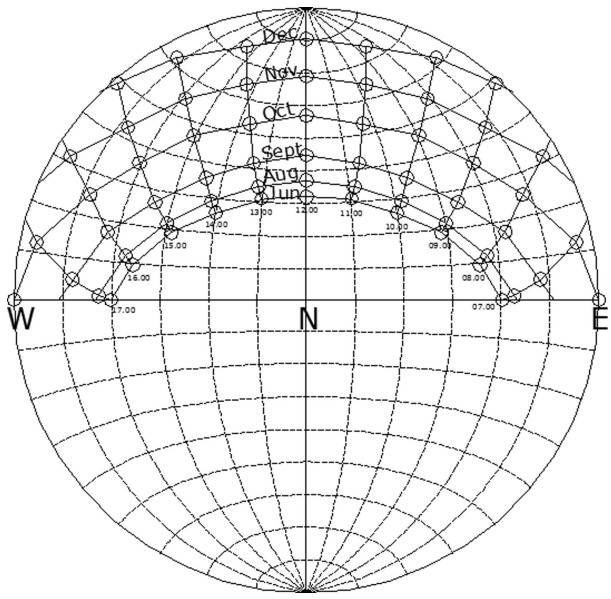

Figure 6 | Analysis grid for the location's sun paths, Latitude: −32°40′

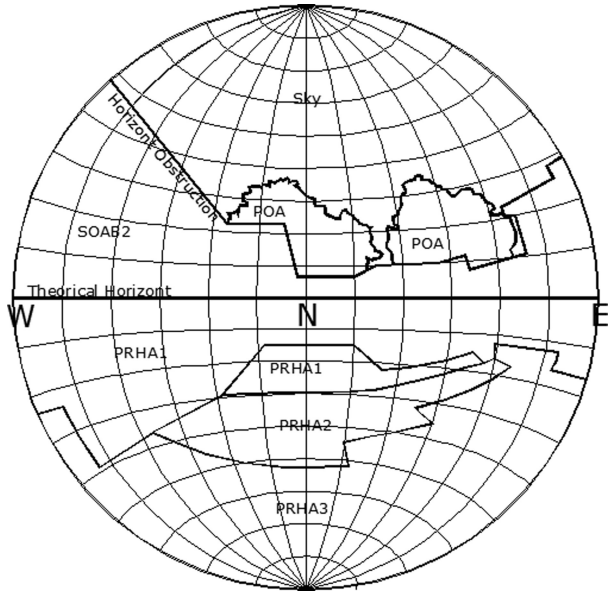

Figure 7 | Synthesis scheme from the analysis of equivalent angular sectors

ANALYSIS OF OBTAINED IMAGES

Once the calculation tool is defined, it is possible to start the image-processing stage.

The objective of this stage is to determine the perceptual participation of the different components of the surrounding environment that have an impact on the availability of solar radiation on a vertical surface in consolidated urban sites. Obstructing and reflecting areas should be assessed for every situation of the environment.

Taking into consideration that on a hemispherical photo image the distance between two points corresponds to an angle, each point corresponds to a coordinate referred to the angular magnitudes of zenith and azimuth of the hemispherical coordinate system. Thus, the area obtained from the image corresponds to an angular area along a hemisphere of directions (Figure 8).

In this manner, the area values obtained from the captured images have a relative value that must be multiplied by the corresponding correction factors in order to determine their real value.

CORRECTING METHOD FOR OBTAINED ANGULAR AREAS

The adjustment (correction) factor method of the obtained angular areas is based on Lynes' theory (Lynes, 1968, Gonçalves de Souza, 2004) on unitary sphere's projection, where the area corresponds to an angular area along a hemisphere of directions. In order to correct the projection's distortion of a three-dimensional section on a plane, a correction factor determined by the author for each section of the hemisphere is utilized (Figures 9 and 10).

DETERMINATION OF THE HORIZON OBSTRUCTION

The line that divides the graphic through its horizontal central axis was defined as the theoretical horizon. The horizon obstruction of a viewpoint is defined as the line that limits the sky-dome obstructions and this can be determined by information collected in the field, orientation and the exact height of each singular point of the silhouette

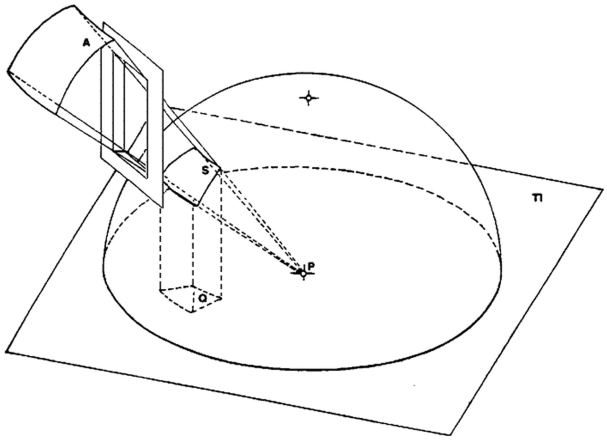

Figure 8 | Scheme of projected solid angle's principle

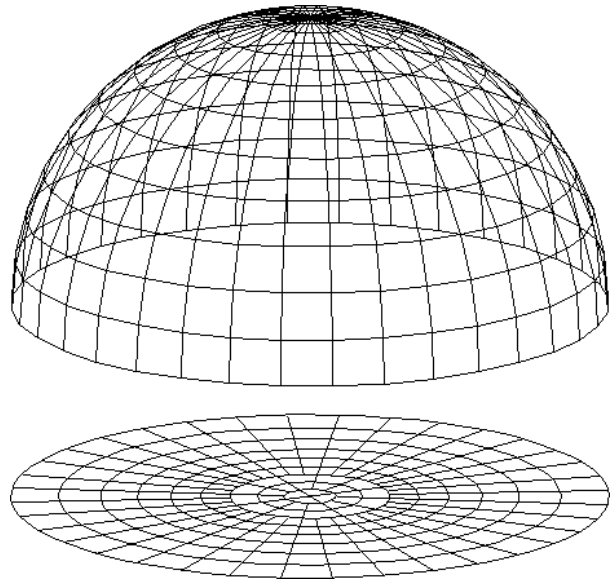

Figure 9 | Stereographic projection of the sky-dome on a bidimensional plane, in 10° sections of altitude and azimuth
Source: Gonçalves de Souza (2004)

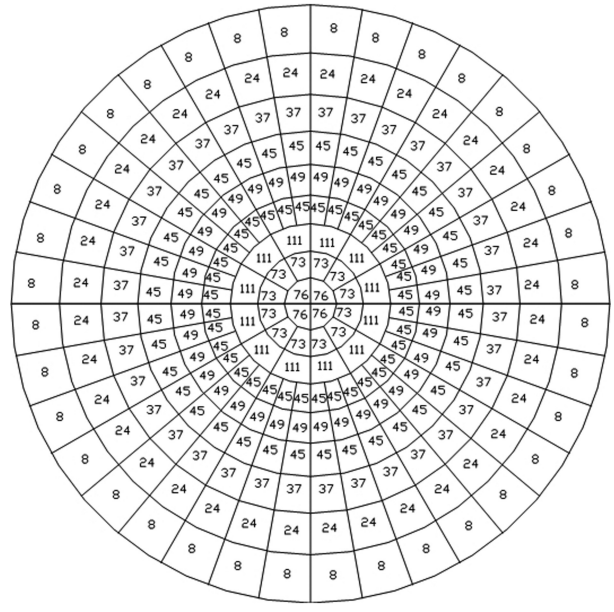

Figure 10 | Quantifying the correction factor of the azimuthally increment for each section of the dome, based on Lynes unitary sphere's theory
Source: Gonçalves de Souza (1997)

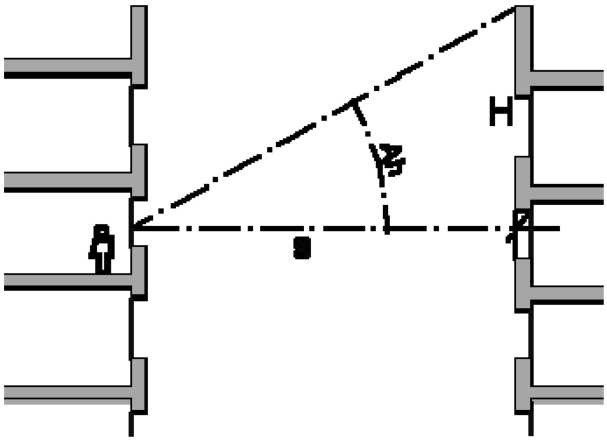

Figure 11 | Trigonometric calculation of height *Ah*

over the horizon. The measurement of each point can be made through graphic or manual means from the height of each singular point to be evaluated, or by analytical means in the case of simulations.

Other methods include using drawings to record the position of each point of the silhouette. By means of a protractor of angles measuring azimuth, *Z*, related to the equator and calculating the height, *Ah*, above the horizon through the relation $\tan Ah = H/S$. *S* is the distance to the point's base and *H* is the point's height related to the observer (Figure 11).

The value of the 'horizon obstruction' is specific for each analysed sector, since when the viewpoint's height varies, so does the incidence of nearby obstructions (Figure 12).

Continuous obstructions along a façade conform to an even height mask, as in the case of faraway mountains, or a continuous planar obstruction, as in a constant height building elevation.

In the two cases analysed in Figure 12, even when the nearby environment is the same, the incidence's percentage of each component is different, in a proportional manner to each one's participation on the hemisphere resulting from the image capture at each point.

A theoretical example of the evaluation of an obstruction due to a continuous masking surface of constant height is presented in Figure 12, as in the case of a uniform height building façade. Because of the distortion caused by the image's type utilized, a continuous façade produces a constant 'obstruction horizon' along the whole image.

In the case of a continuous planar obstruction, as an even run façade across the street, the sky's obstruction would be maximum in the direction perpendicular to the plane and the band that masks the solar paths obstruction by the environment would follow the line of the corresponding angle.

Figure 13 presents the schemes of the continuous obstructions of the cases shown in Figure 12, where it is possible to observe the incidence's variation of an obstacle of constant features in the situation of similar positions.

The mere fact of changing the viewpoint (9 m high) in this case results in significantly different percentages of the sky dome's obstruction, 21.11 and 43.33% in the first and second cases, respectively. When assessing the incidence of these values, it is evident that, in the second case, the direct component of the solar resource will not be available during the season of greater heating demand (June through August). In the early hours of days in the year, conversely, in the first case the resource's availability is reduced only before 8 am and after 4 pm.

Assessing the situation of a multi-storey apartment building (Figure 14), the different heights of the camera determine different obstruction values and the incidence of nearby reflecting surfaces. The capture points' heights were

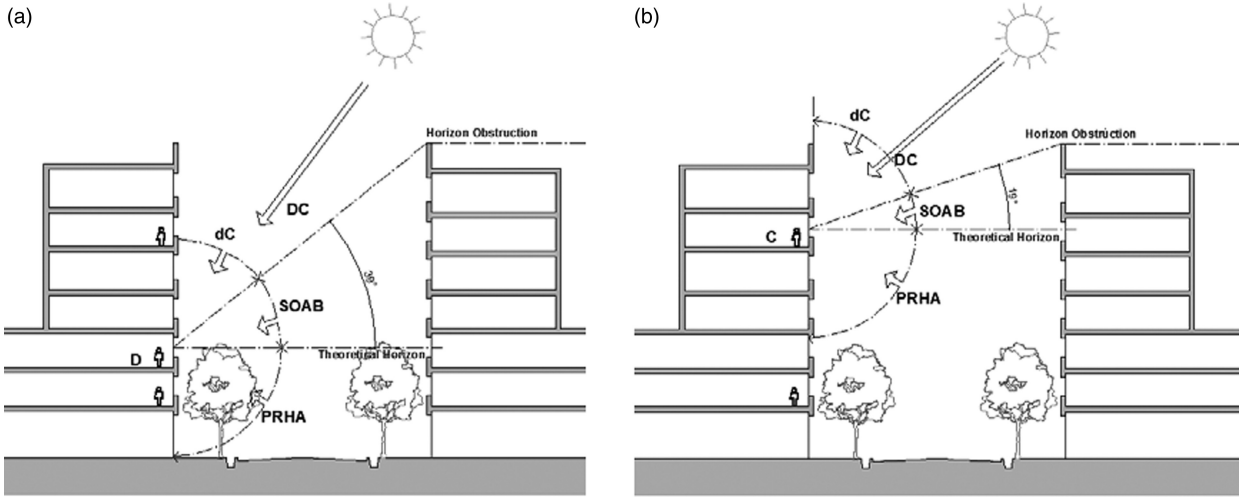

Figure 12 | (a, b) Variation of the incidence of the different components according to the capture's viewpoint

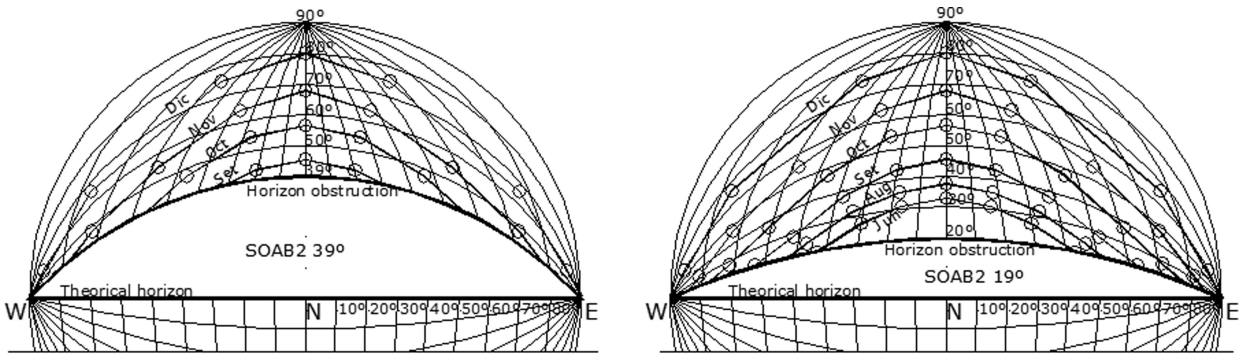

Figure 13 | Mask from the continuous planar obstruction shown in Figure 12, for −32°40′ latitude

sidewalk level (+0.00m), second floor level (+6.00m) and fourth floor level (+12.00m).

The angular area values obtained for each analysed sector are affected by the correction factor. In order to determine their real values from those taken from percentage values for the total hemisphere, the existing correlation between the camera height and the percentage values of the solid obstruction elements (SOAB1, SOAB2 and POA) and the reflecting ones (PRHA) can be verified. The first one maintains a direct relationship (it increases with height) and, conversely, the second one decreases with height. In each case, the variation can reach values higher than 200% (SOAB2), being linear in the case of solid obstructions (15% variation) and in urban forest incidence (POA) (Graphic 1).

ANALYSIS OF MMA'S EXISTING URBAN GRID

In order to test the model's utilization first results, differently featured residential building sectors, representative of different consolidated sectors of MMAs, were analysed.

The considered variables in each case are referred to by their geometric features, which are street and sidewalk width and density and height of nearby constructions. The captured hemispheric images are transformed to synthesis schemes for each assessed environment, using graphic calculation programs (AutoCAD^{R}). From them, the relative areas corresponding to each element can be obtained (solid obstructions, permeable obstructions, reflecting surfaces, etc.). This value, multiplied by the bi-dimensional projection's ponderation factor, yields the percentage relationship of each element's incidence (Figure 15).

The calculation of the impinging radiation values on a vertical surface, as assessed in Figure 15, provides a more direct notion of the urban forest's incidence on solar availability. In the mentioned example the obstruction of the green mask is almost total, hence the importance of the adequate selection of tree species. In the same example, the incidence of using different tree species is evaluated, considering the case of a non-existing forest for the three seasonal periods of greater space heating demand, considering the radiation values of the 12 diurnal hours (Table 1, Graphic 2).

The forest's incidence on the potentially impinging solar radiation in the analysed case demonstrates the importance of an adequate choice of arboreal species in the urban environment. During the winter season, in the most favourable case, the available radiation values drop by more than 50%, because of the incidence of the 'vegetal filter'. In turn, similar obstruction percentage values can be observed for the different tree species evaluated.

The results obtained from the studied cases have been structured to determine, for each plane, areas of solar obstruction as a function of the nearby environment's morphology. The percentage values of solar radiation obstruction hours due to the environment were obtained. The reflecting areas, according to their position, material and, in the case of urban trees, their morphological and permeability features, were quantified.

ANALYSIS SECTORS SELECTION

The selection of urban sectors for the study was based on their homogeneity relative to all the considered indicators to be assessed, which assumes a similar range in behaviour, making their adoption as operational units possible.

Through field studies, supported by the analysis of maps and satellite images, five study sectors have been selected, based on the geometric features of urban canyons and the built units' morphology (high- and low-density city-blocks), belonging to the Capital and Godoy Cruz municipalities.

Sector 1 (street width: 20.00m, low building density, first magnitude urban trees)The sector represents 35% of MMA's total urban canyons, their key features being shape, age and species of the existing urban trees, buildings not higher than two storeys and values of sealed soil on causeways and sidewalks higher than 90% (Figure 16 and Table 2).

Sector 2 (street width: 20.00m, high building density, first magnitude urban trees)

Because of the geometric features of the grid, the essential difference between the preceding case and this case is

Image capture: level +0.00m

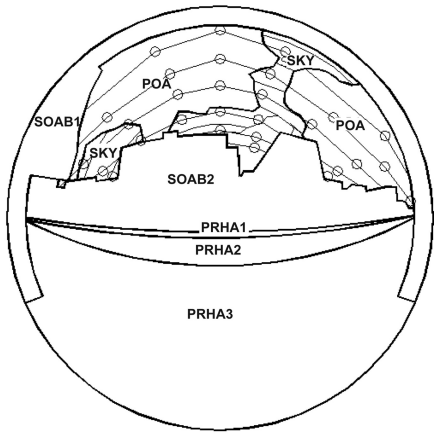

Synthesis scheme: level +0.00

Image capture: level +6.00m

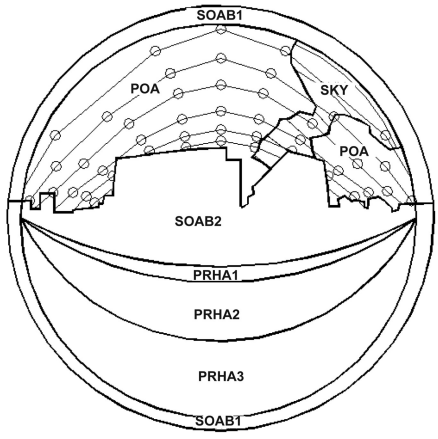

Synthesis scheme: level +6.00

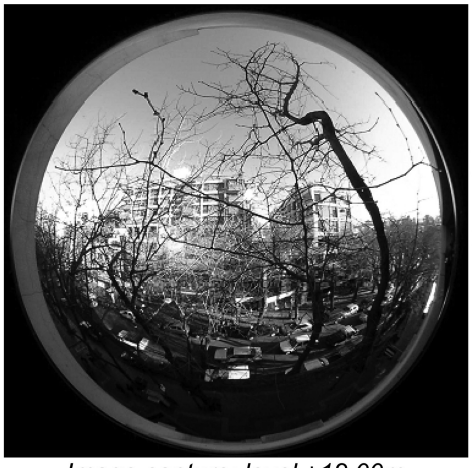

Image capture: level +12.00m

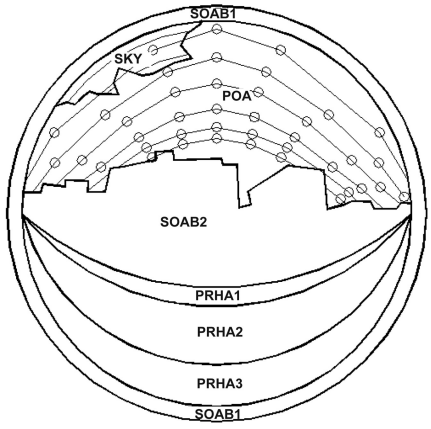

Synthesis scheme: level +12.00

Figure 14 | Obstructions evaluation of high-density areas of MMA

the surrounding environment's building density. Constructions higher than eight storeys surround the place, giving it special features; the existing tree set is homogeneous and the percentage values of sealed soil on causeways and sidewalks are higher than 90% (Figure 17 and Table 3).

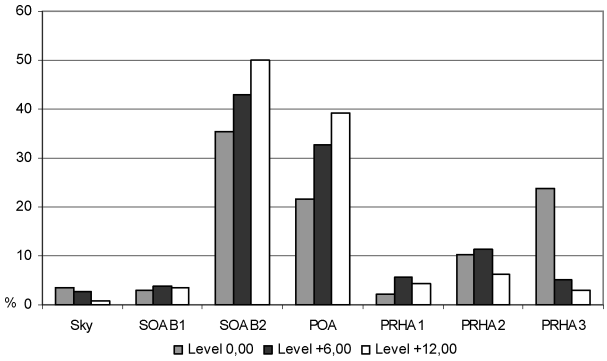

Graphic 1 | Percentage results from analysis

Sector 3 (street width: 30.00m, low building density, first magnitude urban trees)

This represents 30% of the urban canyons in MMA. Their main features are given by the separation between built front walls, which would lead to better morphological features for solar access of the same. The existing tree set is homogeneous as to form, age and species; the buildings are not higher than three storeys and percentages of sealed soil on causeways and sidewalks are higher than 90% (Figure 18 and Table 4).

Sector 4 (street width: 30.00m, high building density, first magnitude urban trees)

The sector represents a minimum percentage in MMA; given its high building density feature, the tree set is homogeneous to the predominance of a single species and its individual's development.

It is located at the microcentre area of the municipal Capital city, framed by light-coloured high-rise constructions. Its sealed soil areas amount to 100% of the total, and the paved areas are homogeneous as far as materials and colours are concerned. This is mainly because it is a commercial area of exclusive pedestrian circulation (Figure 19 and Table 5).

Sector 5 (street width: 14.00m, low building density, second magnitude urban trees)

Alleyways narrower than 16m represent 23% of the total urban canyons in MMA. In this specifically evaluated case, the main features are the scarce presence of urban trees, with buildings not higher than two storeys, and a 100% sealed soil of causeways and sidewalks (Figure 20 and Table 6).

Digital Image

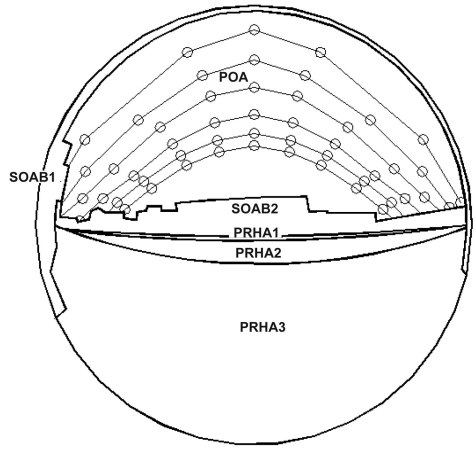

Analisys` synthesis scheme

Figure 15 | Case of analysis: low-density area, street width 30.00m

Table 1 | Seasonal values of hour irradiance for the tree species in urban conditions

Season	Tree species				Without trees	
	London plane	White mulberry	European ash	China berry		
Fall	0.46	0.60	0.50	0.73	3.32	Hour irradiance (Mj/m^{2}h)
Winter	1.61	2.42	1.81	3.09	6.71	
Spring	1.11	1.20	0.38	1.41	2.93	

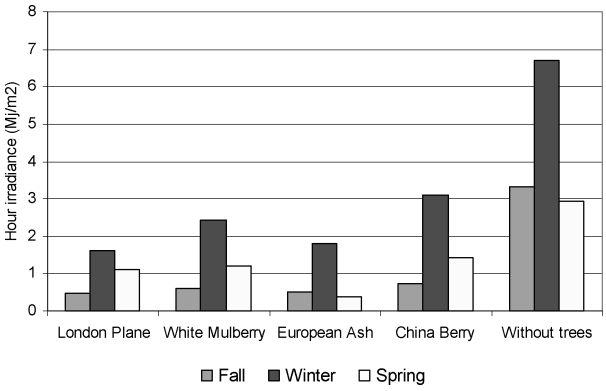

Graphic 2 | Seasonal values of hour irradiance

RESULTS

The first results obtained are representative of each one of the selected sectors and offer a precise characterization of the evaluated indicators' incidence on each sector's solar potential (Graphic 3).

In the analysed cases, the results are not similar, as a consequence of each area's geometric features. They maintain, however, a logic correlation on the incidence's variation of each indicator. In most cases, the visible sky free of obstructions (solid and permeable) is minimum or nil, with the exception of Case 5, where, given its low-density features and the almost zero presence of urban trees, the potential use of solar energy is very high. The nearby reflecting surfaces (PRHA1/2/3) present a high participation in the total percentages (variations from 25 to 37%), thus indicating the need to treat those surfaces to control their incidence. The urban trees' participation in the obstructions (POA) is maximum in sectors 1 and 3, reaching values higher than 40%; in the first four sectors however, the existing species are homogeneous, which allows easing of the incidence's assessment of the 'green curtain'. The results obtained for indicator POA, affected by the seasonal blockage's percentage values (intrinsic of each species), allowed the obtainment of effectively shaded areas (Cantón *et al.*, 2003). These results confirm the importance of considering the species utilized, to avoid obstructions in the season when high solar permeability is required.

The incidence of the nearby building's height presents obstruction variations ranging from 15% for lower densities to over 43% for higher ones. The street width related to the building height has an average obstruction incidence of 5% (Sectors 2 and 4).

In all cases the percentage values corresponding to potentially reflecting surfaces is close to 45% (PRHA indicators).

Further studies in this field will be aimed at determining the real values of the reflected component due to nearby horizontal reflecting surfaces to develop technical strategies for the appropriate treatment of such surfaces' reflective features in order to accomplish the objectives set forth.

Figure 16 | Sector 1 images

Table 2 | Sector 1 material features.

Sector	SOAB1	SOAB2	POA	PRHA1	PRHA2	PRHA3
1	Not present	Various colour of vertical walls	Species: mulberry	Cement tiles various colours	Concrete	Cement tiles various colours

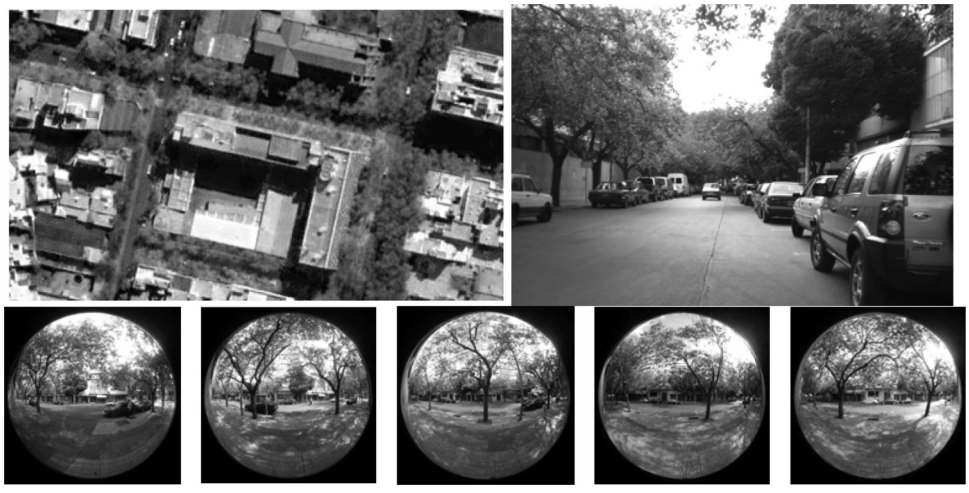

Figure 17 | Sector 2 images

Table 3 | Sector 2 material features (idem Sector 1)

Sector	SOAB1	SOAB2	POA	PRHA1	PRHA2	PRHA3
2	Not present	Various colour of vertical walls	Species: mulberry	Cement tiles various colours	Concrete	Cement tiles various colours

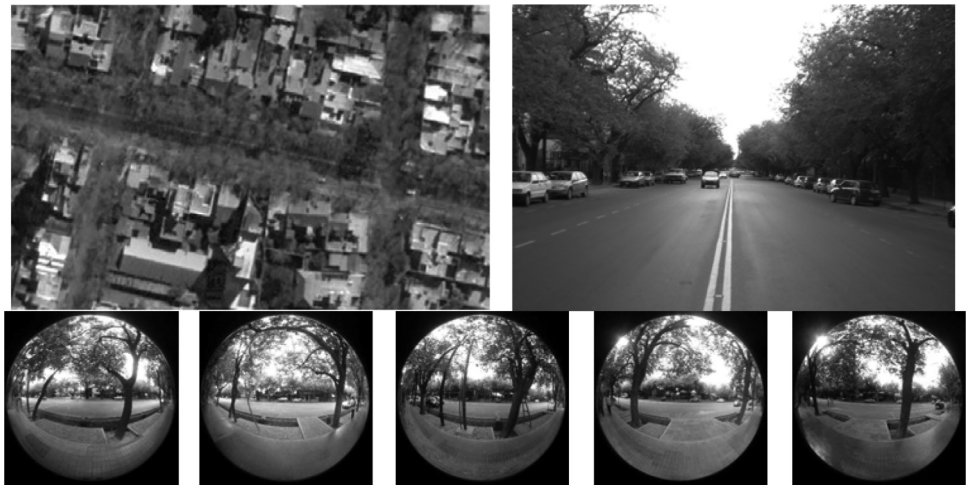

Figure 18 | Sector 3 images

Table 4 | Sector 3 material features

Sector	SOAB1	SOAB2	POA	PRHA1	PRHA2	PRHA3
3	N/A	Low vertical walls of various colours	Species: mulberry	Cement tiles various colours	Concrete	Cement tiles various colours

Figure 19 | Sector 4 images

Table 5 | Sector 4 material features

Sector	SOAB1	SOAB2	POA	PRHA
4	Commercial overhangs	Light coloured tall outer walls	Species: mulberry	Dark coloured concrete pavers

Figure 20 | Sector 5 images

Table 6 | Sector 5 material features

Sector	SOAB1	SOAB2	POA	PRHA1	PRHA2	PRHA3
5	Not present	Varied coloured low-rise outer walls	Few individuals various species	Cement tiles various colours	Concrete paving	Cement tiles various colours

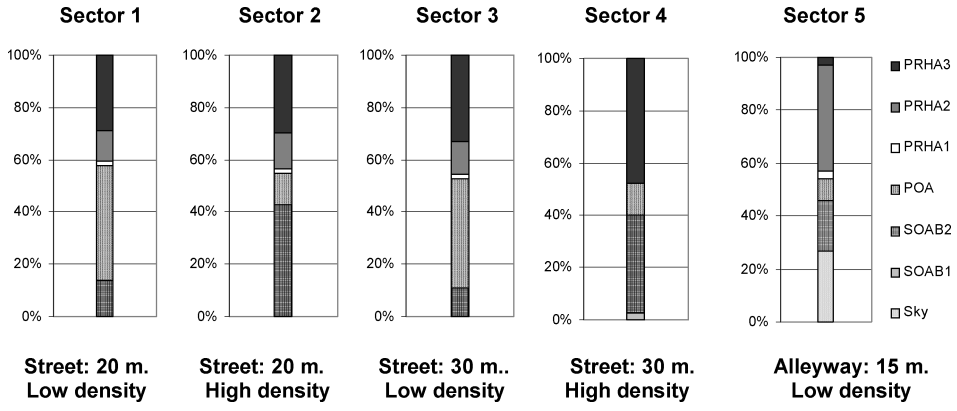

Graphic 3 | Mean results from each sector's assessment

CONCLUSIONS

The analysis methodology presented is an easy-to-use tool, which offers precise assessment results of urban environments with features which make them difficult to evaluate by other means.

The utilization of the obtained results from the analysis of different sectors in the city (hours of available radiation, obstruction periods and elements that cause them, opaque and permeable, reflective surface's incidence) will allow us to determine, in each case, according to their morphological and constructive features, the incidence of each component of incoming solar radiation on buildings' outer walls and windows. Thus, feeding the results to the development of normative guidelines aimed at the most efficient use of renewable energy resources in urban buildings.

In order to complete the results obtained in this study, it is foreseen, in a further stage, that one should develop a database of the most common types of building technology in the region for sealed soil of public open spaces (causeways and walkways), their thermal and reflective properties and, in this way, adjust the available knowledge on the radiative and thermal processes within city environments.

References

Cantón, M.A., Cortegoso, J.L. and de Rosa, C., 2001, 'Environmental and energy impact of the urban forest in arid zone cities', *Architectural Science Review* 44(1), 3–16.

Cantón, M.A., Cortegoso, J.L. and de Rosa, C., 1994, 'Solar permeability of urban trees in cities of western Argentina', *Energy and Buildings* 20(3), 219–230.

Cantón, M.A., Mesa, A., Cortegos, J.L. and de Rosa, C., 2003, 'Assessing the solar resource in forested urban environments results from the use of a photographic-computational method', *Architectural Science Review* 46(2), 115–124.

Correa, E., Pattini, A., Córica, M.L., Fornés, M. and Lesino, G., 2005, 'Evaluación del factor de visión de cielo a partir del procesamiento digital de imágenes hemisféricas. Influencia de la configuración del cañón urbano en la disponibilidad del recurso solar'. *Avances en Energías Renovables y Medio Ambiente* 9, Argentina.

Córica, L. and Pattini, A., 2006a, 'Study of diffuse and reflected components to daylighting potential in urban environments of high and low density in Mendoza, Argentina', *24th Conference on Passive and Low Energy Architecture, Passive and Low Energy Architecture PLEA – Universidad de Geneva, Geneva, Switzerland.*

Córica, L. and Pattini, A., 2006b, 'Permeabilidad lumínica urbana: factor de visión de cielo en recintos urbanos característicos de la ciudad de Mendoza', *VIII Congreso Panamericano de Iluminación-Luxamerica 2006*, *Audi - Asociación Uruguaya de Iluminación, Montevideo - Uruguay*.

Córica, L. and Pattini, A., 2007, 'Evaluación comparativa de distribución lumínica en recintos urbanos de la ciudad Mendoza. Estación estival. Encac- Elacac 2007', *IX Encontro nacional e V Latino Americano de conforto no ambiente construido, Ouro Preto*.

Gonçalves De Souza, R., 1997, 'Iluminação Natural em Edificações: cálculo de iluminâncias internas desenvolvimento de ferramenta simplificada', Curso de Pós-Graduação em Engenharia Civil da Universidade Federal de Santa Catarina, como parte dos requisitos para obtenção do título de Mestre em Engenharia Civil.

Gonçalves De Souza, R., 2004, 'Desenvolvimento de modelos matemáticos empíricos para a descrição dos fenômenos de iluminação natural externa e interna', Tesis Doctoral, UF de Santa Catarina Programa de Pós Graduação.

Hay, J., 1979, 'Calculation of monthly mean solar radiation for horizontal and inclined surfaces', *Solar Energy* 23, 301.

Klucher, T.M., 1979, 'Evaluation of models to predict insulation on tilted surfaces', *Solar Energy* 23(2), 111–114.

Lynes, J.A., 1968, *Principles of Natural Lighting*, USA, Elsevier Publishing Company.

Martinez, C.F., Córica, L., Endrizzi, M., Pattini, A. and Cantón, M.A., 2006, 'Effect of urban forest on daylight availability in built environments. The

case of Metropolitan Area in Mendoza', *Plea 2006 – The 23rd Conference on Passive and Low Energy Architecture, Passive and low energy architecture – Universidad de Geneva – Hes-so. Geneva, Switzerland*.

Mesa, N.A., de Rosa, C. and Cortegoso, J.L., 2000, 'Determinación del área de fachadas potencialmente colectoras, en medios urbanos, a través de un modelo gráfico computacional', *Ponencia. ISES Millennium Solar Forum 2000*, *México, Setiembre de 2000*.

Randall, S.F., Gerding, R.B., O'Rourke, P.A. and Terjung, W.H., 1981. 'An urban radiation obstruction model', *Boundary-Layer Meteorology* 20(2), 259–264.

Robinson, D., Stankovic, S., Morel, N., Deque, F., Rylatt, M., Kabele, K., Manolakaki, E. and Nieminen, J., 2003, 'Integrated resource flow modelling or urban neighbourhoods: project SUN tool', *Proceedings of the Eighth International IBPSA Conference on 'Building Simulation 2003', Eindhoven, Netherlands, 11–14 August 2003*, 1117–1122.

Robinson, D. and Stone, A., 2004, 'Solar radiation modelling in the urban context', *Solar Energy* 77(3), 295–309.

Roxburgh, J.R. and Kelly, D., 1995, 'Uses and limitations of hemispherical photography for estimating forest light environments', *New Zealand Journal of Ecology* 19(2), 213–217.

Temps, R.C. and Coulson, K.L., 1977, 'Solar radiation incident on slopes of different orientation', *Solar Energy* 19(2), 179–184.